Supporting Information for:

Functional polyethylene glycol based solid electrolytes with enhanced interfacial compatibility for room-temperature lithium metal batteries

Yuhang Zhang[a], Shimou Chen[b, c]*, Yong Chen[d], and Lingdong Li[a,]*

[a]School of Chemical Engineering, Dalian University of Technology, Panjin 124221, China.

[b] Beijing Key Laboratory of Ionic Liquids Clean Process. Institute of Process Engineering, Chinese Academy of Sciences, Beijing 100190, China.

[c] State Key Laboratory of Chemical Resource Engineering, Beijing University of Chemical Technology, Beijing, 100029, China.

[d] School of Chemical & Environmental Engineering, China University of Mining & Technology, Beijing 100083, China.

Corresponding author E-mail: chenshimou@ipe.ac.cn (S. M. Chen); lild@dlut.edu.cn (L. L. Li).

1. Experiments

1.1. Material Characterizations

The structure and polymerization of SPEs were characterized by Fourier Transform infrared spectrometers (FTIR). The thermal properties of SPEs were characterized by thermogravimetric analyzer (TGA, Setaram Labsys) with a heating rate of 5 °C min^{-1} from 25 °C to 600 °C and a Differential Scanning Calorimeter (DSC) with a heating rate of 5 °C min^{-1} from -80 °C to 80 °C. The X–ray diffractometer (XRD, Bruker D8 Focus) with a Ni–filtered Cu Kα radiation (λ = 0.15406 nm) source was used to analyze the crystalline state of SPEs. The scanning electron microscope (SEM, Haitich SU8020, Japan) with a 5-kV acceleration voltage was carried out to characterize the morphology and structure of anode and cathode materials. Elemental mappings of SPEs were obtained using EDS related to the SEM.

1.2. Electrochemical measurements

The ionic conductivities of SPEs were determined with 2025 type coin sandwiching the in-situ SPEs between two stainless steel. The electrochemical impedance spectroscopy (EIS) measurements were carried out with 10 mV of AC amplitude over the frequency range from 0.1 Hz to 0.1 MHz. The following equation Eq.(1) was used to calculate the ionic conductivity of SPEs. Where L is the thickness of SPEs, S is the effective area and the R is the bulk resistance of SPEs. The calculated ionic conductivities were consistent with Vogel–Tamman–Fulcher (VTF) empirical equation with different temperatures as Eq.(2).

$$\sigma = \frac{L}{S\,R} \tag{1}$$

$$\sigma = AT^{-1/2} exp\left(\frac{-E_a}{k(T - T_0)}\right) \tag{2}$$

The lithium ion transference numbers (t_{Li+}) of SPEs were tested on a 2025 type

coin sandwiching the in-situ SPEs between two Li by AC impedance and DC polarization. Where the polarization currents (initial (I_0) and steady-state (I_{ss})) were measured under a DC polarization voltage of 20 mV (ΔV). The impedances before and after polarization are R_0 and R_{ss} ,respectively. Then the t_{Li+} was calculated according to Bruce–Vincent–Evans equation as Eq.(3).

$$t_{Li+} = \frac{I_{ss}(\Delta V - I_0 R_0)}{I_0(\Delta V - I_{ss} R_{ss})} \quad (3)$$

The compatibility with Li-anode was showed by the following experiments. The interface impedances changing with time were tested after 0, 1, 5, 10, 15, 20, 30 days. The lithium plating−stripping galvanostatic cycling performances of Li/SPEs/Li symmetric cell under 0.2 mA/cm^2 and rate performances under different current densities (0.1, 0.2, 0.3, 0.4, 0.5, 1 mA/cm^2) were conducted. The assembled Li/PPEVS/$LiFePO_4$ (1 C = 170 mA h/g) cells were tested between 2.5 V to 4.2 V for cycling and rate performances after the cells ran for three cycles at low rate (0.1 C) to ensure the gradual formation of stable SEI layers and the full polymerization of the polymer precursors. Linear sweep voltammetry curves of Li/PPEVS/stainless-steel asymmetric cell were performed by an electrochemical workstation (Autolab 304N) at a scanning rate of 0.1 mV/s. Cyclic voltammetry curve of Li/PPEVS/$LiFePO_4$ was performed by an electrochemical workstation at a scanning rate of 0.1 mV/s with a scan from 2 V to 4.2 V. The above tests were at ambient temperature.

2. Supplementary Figures

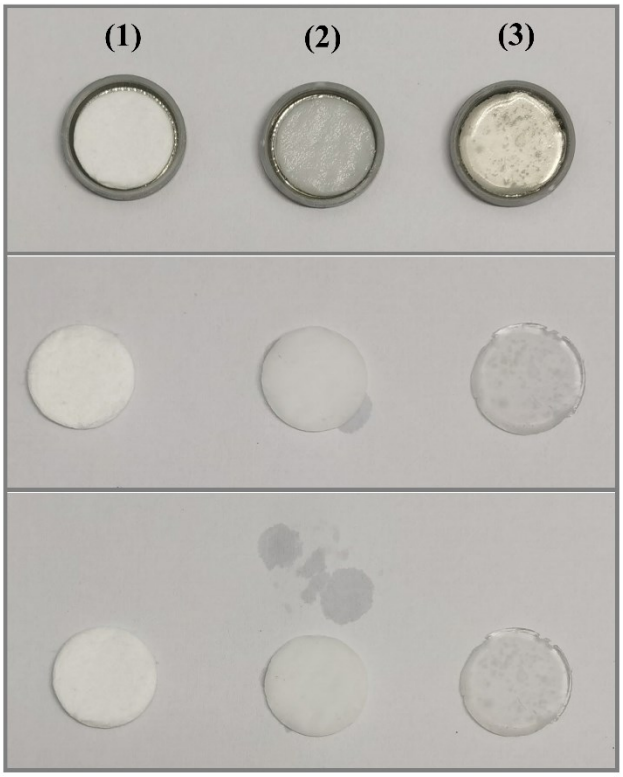

Figure S1. Appearance photography of three membranes from disassembled batteries based on (1) pure glass fiber (GF), (2) GF-PEGDMA-VC and (3) GF-PPEVS

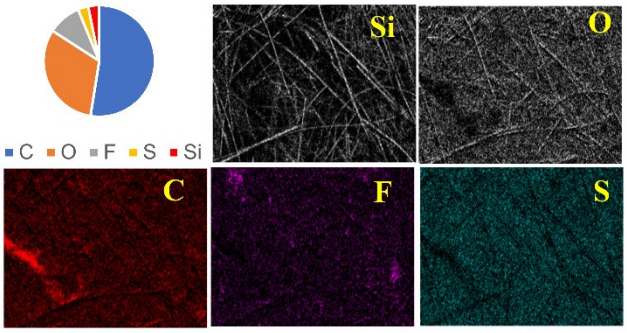

Figure S2. Energy dispersive spectroscopy mappings related to surface morphology of GF-PPEVS from the disassembled cells.

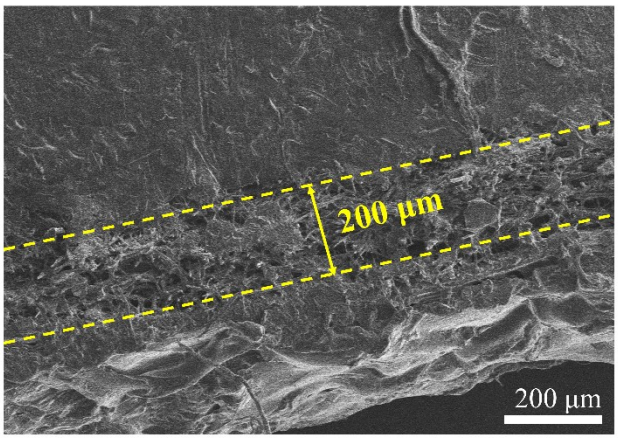

Figure S3. Cross-section morphology of Li/PPEVS/$LiFePO_4$ from the disassembled cells after in-situ polymerization.

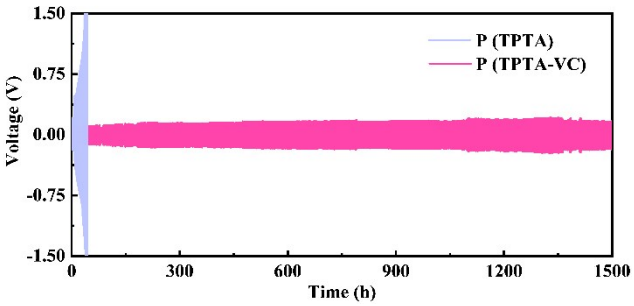

Figure S4. Li plating/stripping cycle performance of Li/P(TPTA)/Li and Li/P(TPTA-VC)/Li symmetrical cells.

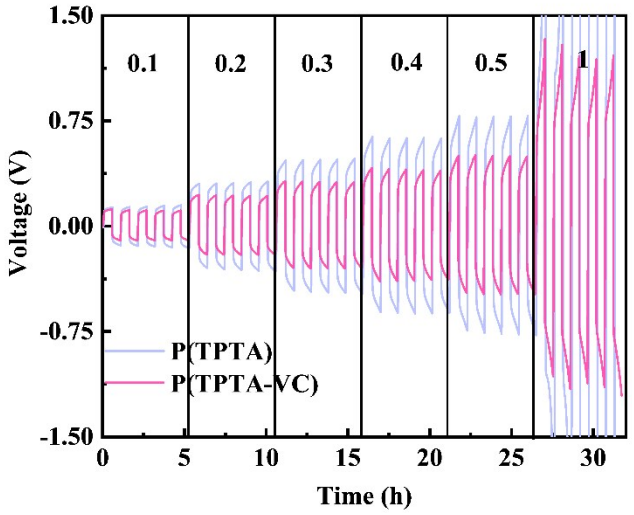

Figure S5. Li plating/stripping C-rate performance of Li/P(TPTA)/Li and Li/P(TPTA-VC)/Li symmetrical cells.

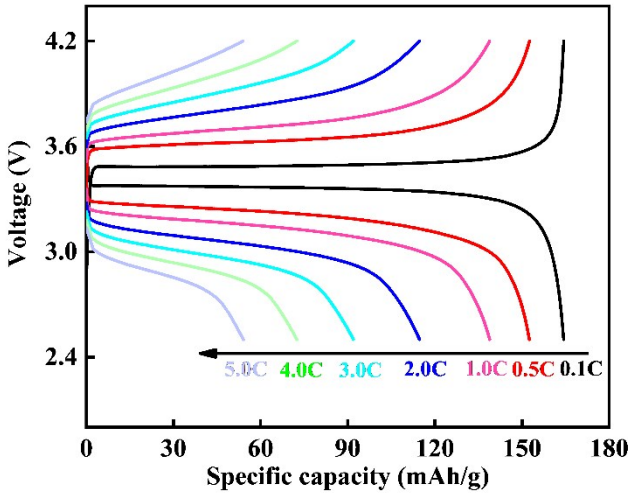

Figure S6. Charge and discharge curves of Li/PPEVS/$LiFePO_4$ at different C-rates.

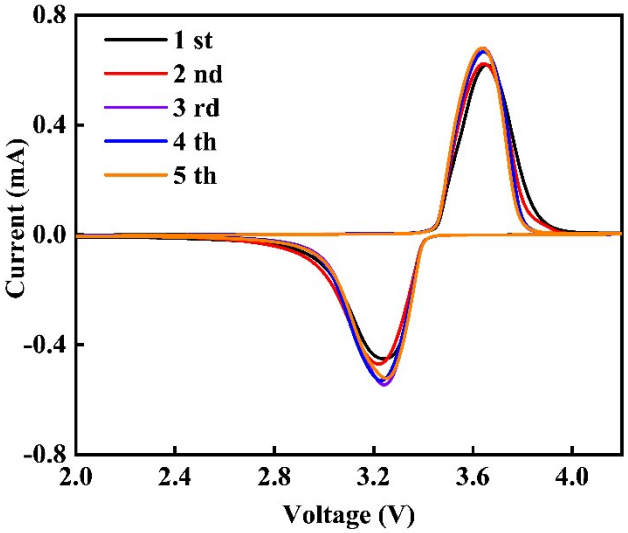

Figure S7. Cyclic voltammetry curve of Li/PPEVS/$LiFePO_4$.

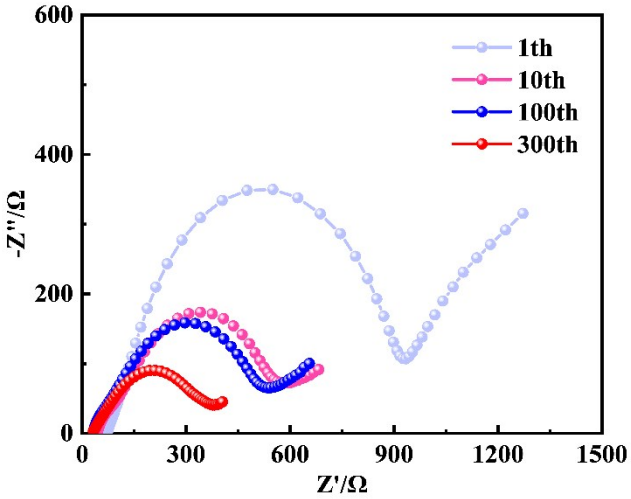

Figure S8. AC impedance spectra of Li/PPEVS/LiFePO4 at different cycles.

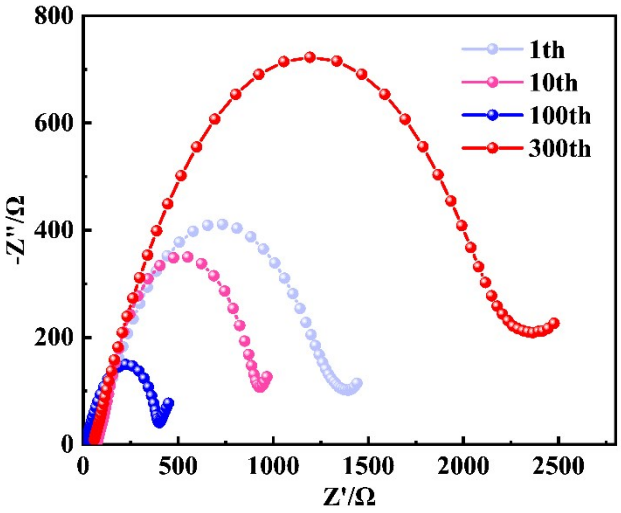

Figure S9. AC impedance spectra of Li/PPEAS/LiFePO4 at different cycles.

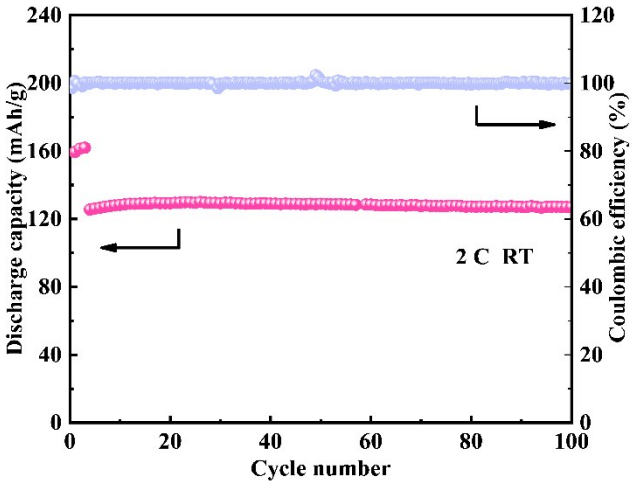

Figure S10. Cycling performances of Li/PPEVS/$LiFePO_4$ cells at 2 C at ambient temperature.